Neutron-antineutron oscillations beyond the quasifree limit

E. David Davis[*] and Albert R. Young[†]

*Department of Physics, North Carolina State University, Raleigh, North Carolina 27695-8202, USA
and Triangle Universities Nuclear Laboratory, Durham, North Carolina 27708-0308, USA*
(Received 22 November 2016; published 8 February 2017)

Prompted by plans for a free neutron oscillation experiment at the European Spallation Source (ESS), we consider issues associated with the magnetic fields that must be present. To this end, we introduce a stochastic model of the residual magnetic field within the propagation region which draws on features of magnetic profiles measured during the last free oscillation experiment at the Institut Laue-Langevin (ILL). A perturbative analysis, which relates the antineutron probability to the power spectral density of the magnetic field sampled, suggests that deviations from the quasifree result will increase quadratically with the length l of the propagation region. However, with inclusion of averaging over representative spectra of neutron speeds, departures from the quasifree result are found to be approximately linear in l. As regards the large spikes in the magnetic field at, for example, joints in the magnetic shielding of the propagation region (despite compensating currents and magnetic idealization of the shield), we demonstrate that their effect scales as $l/D^{3/2}$, where D is the diameter of the cylindrical magnetic shielding, and identify conditions under which they can be neglected. We also establish that any large magnetic field encountered after the propagation region is exited will not diminish the probability for antineutron detection. For the range of values of l of most interest to the ESS experiment, it should suffice to improve on the level of magnetic suppression achieved at the ILL by a factor of 2.

I. INTRODUCTION

With construction of the European Spallation Source (ESS) [1] in Lund, Sweden, there is renewed interest [2–5] in an experimental study of free neutron-antineutron oscillations that would improve on the work done at the Institut Laue-Langevin (ILL) in the 1990s [6,7], which, in turn, superseded earlier experiments [8–10]. As highlighted in the historical overview in Ref. [11], the search for neutron-antineutron oscillations would complement that for neutrinoless double beta decay. Both phenomena violate the "accidental" global anomaly-free Standard Model (SM) symmetry resulting in conservation of the difference between the baryon number B and the lepton number L. If the example of the SM has anything to teach us, it is that the identification of apposite symmetries is key to successful model building: thus, the status of this $(B - L)$ symmetry [12,13] is important, and the *observation* of neutron-antineutron oscillations [involving $|\Delta(B - L)| = 2$ transitions] would be a discovery of physics beyond the Standard Model (or BSM physics). Furthermore, the detection of neutron-antineutron oscillations along with either a B- or a $(B - L)$-violating nucleon decay would imply [14] that neutrinoless double beta decay must occur. Of course, there is a more direct link between neutron-antineutron oscillations and neutrinoless double beta decay within models [15] that postulate spontaneous breaking of

the global $U(1)_{B-L}$ symmetry. In their own right, neutron-antineutron oscillation studies are an avenue to information on $|\Delta B| = 2$ processes which can drive postsphaleron baryogenesis [16–20] and may contribute to an explanation of the observed baryon asymmetry of the universe. It has also been argued that, in view of their sensitivity to any difference in neutron and antineutron rest energies, neutron-antineutron oscillation experiments with free neutrons furnish a potentially stringent test of Lorentz invariance [21] and, in similar vein, that discovery of neutron-antineutron oscillations would impose strong limits on any departure from the equivalence principle [22]. There have been formal arguments [23–26] attempting to identify a role for CP violation in neutron-antineutron oscillations, but the model-dependent considerations of Ref. [27] suggest that it would be very small (although oscillations of heavy flavor baryons could exhibit substantially more CP violation).

Models giving rise to neutron-antineutron oscillations date back (with the notable exception of Ref. [28]) to the end of the 1970s, some of the pioneering papers being Refs. [29–42]. The advent of the Large Hadron Collider (LHC) has prompted an understandable emphasis on models with predictions which are testable at mass scales of 1 TeV/c^2 or so (for the most up-to-date reviews, see Refs. [4,43] or, for a broader perspective, Ref. [44], which relies heavily on Refs. [45,46] in its discussion of neutron-antineutron oscillations). Despite the impending avalanche of LHC data on rare processes, a case is made in Ref. [4] that the ESS-based effort to increase the lower bound on the

---
[*]dedavis4@ncsu.edu
[†]aryoung@ncsu.edu

036004-1

neutron-antineutron oscillation rate will be useful. This claim has been substantiated by a study [47] of simplified supersymmetric (SUSY) models with R-parity violation, which include $|\Delta B| = 2$ processes and can accommodate the absence of SUSY signatures in run 1 of the LHC: even after allowing for uncertainties [48] in hadronic matrix elements of B-violating interactions (which are being addressed by the lattice QCD community [49–51]), it is concluded that, for certain regions of the model parameter spaces, the projected ESS experiment can probe for gluino and squark masses at energies beyond the foreseeable reach of the LHC program as well as other BSM searches based on flavor transitions, CP violation, and dinucleon decays. Given the increasing number of models [52–61] which imply the possibility of observable neutron-antineutron oscillations, the more experiments performed the better.

In the mold of the ILL example, the current conception of the next generation of free oscillation experiments envisages a high flux of slow neutrons propagating down a long, horizontal, magnetically shielded, and evacuated cylinder ("the propagation region") to a target surrounded by an antineutron annihilation detector. Unique among experiments looking for B violation, this setup offers the possibility of high sensitivity freed of significant backgrounds. The hope is that with a dedicated beam line, advances in neutron moderator technology, modern neutron optics, and a longer propagation region, the ILL limit on the free neutron oscillation probability can be bettered by at least 3 orders of magnitude.

In the latest assessment (conducted in Ref. [4]) of future n-n̄ oscillation experiments, it is suggested on the basis of a rough estimate that "one requires a magnetic field in the 1–10 nT regime to meet the quasi-free condition" and there is a call for "a significant research program to understand how to achieve this lower limit [on the magnetic field] in a cost effective manner, and to understand the possible reduction in sensitivity that might arise from residual field configurations." (The quasifree condition is tantamount to the requirement that, for the passage through the propagation region, the difference in neutron and antineutron energies is much less than the limit set by the energy-time uncertainty principle.) The present paper represents a partial response to this challenge.

Our treatment of the residual magnetic field is based on an extension of the 4-state (or vector) model in Ref. [62] to accommodate random inhomogeneities. Inhomogeneities are perforce present when mumetal magnetic shielding is in place, because external magnetic fields, which are otherwise excluded, enter where segments of the shield are mechanically joined together [63,64]. Comparison of magnetic field profiles recorded during the ILL experiment [65] points to the existence of unpredictable changes in inhomogeneities during runs and following the regular magnetic idealizations [63] of the shielding. By viewing the

inhomogeneities as random, an interrelated effect can be incorporated, namely, the different values of the magnetic field experienced by neutrons on neighboring flight paths through the propagation region. Differences in the magnetic field across a cross section of the propagation region are due to inhomogeneities in the nonaxial (or transverse) components of the field, which result from the increases in the longitudinal field at points along the shield where there are magnetic "leaks." There are also random fluctuations with time in the ambient field although it has been past practice to compensate for these (whatever their source) by an active feedback system [63]. An average over the ensemble of neutrons studied during the course of a many-year experiment involves implicitly an average over all of the values of the actual field sampled.

A stochastic analysis of the effect of magnetic field on neutron-antineutron oscillations is clearly not needed if field profiles have been measured. The measured profiles themselves can be used in conjunction with numerical solutions of Schrödinger's equation to determine the extent to which oscillations have been suppressed. However, our stochastic approach permits discussion of the design of an experimental setup in the planning stage for which there is, perforce, no actual magnetic profile data.

In this paper, a number of topics related to generic aspects of the residual magnetic field are addressed. Paramount is the issue of whether, as suggested in Ref. [4], the acceptable size of the residual magnetic field in future experiments must be as low as 1 nT on average (i.e., about a factor of 5 smaller than the average field in the ILL experiment). What, if any, is the cumulative impact of small unavoidable inhomogeneities in the field given the increased length of the propagation region to be used (maybe as much as nearly 3 times as long as that in the ILL experiment [4])? The relation between the limit on the magnetic field and propagation distance has not been broached explicitly before but should be quantified. Another consequence of increasing the length of a mumetal shield which does not seem to have been given any attention (in the context of ILL-type experiments) is the increasing strength of spikes in the field [64] at magnetic leaks in the shielding. Even with carefully adjusted compensating currents (aimed at achieving cancellations accurate to more than one part in 2000), large peaks (~ 0.1 μT) usually persist at a handful of joints near the ends of the magnetic field profiles recorded during the ILL experiment (see, for example, Fig. 13 in Ref. [63]). The dependence of these features on the length of the shield is nonlinear (approximately quadratic). Thus, although the effect of these abrupt variations in the field was discounted in the analysis of the ILL experiment, their presence could be more significant for an experiment with a longer shield. There is also the large magnetic field in the region between the end of the mumetal shield and the annihilation detector to be considered.

In our stochastic model of the magnetic field, we distinguish between the large spikes in the field and the otherwise small residual field. The latter is treated perturbatively, and its random behavior (in the rest frame of any neutron) is assumed to be wide-sense stationary [66], in view of the presence of compensating currents designed both to iron out inhomogeneities along the full length of the propagation region and to actively counteract any time dependent fluctuations. Our treatment of the large spikes is such that we do not have to commit ourselves to any detailed specification of their statistics.

The structure of the paper is as follows. Section II begins with the 4-state model for neutron-antineutron oscillations as formulated in Ref. [62], and then presents a perturbative result for the antineutron probability which includes the effect of small random inhomogeneities in the residual field (or magnetic noise). In Sec. III, numerical estimates of the effect of this magnetic field noise on the quasifree propagation efficiency η for new ILL-type experiments are given, with particular attention being paid to dependence on the length of the shielded neutron propagation region. The impact of large fields at leaks in the shielding and at the end of the propagation region, in the vicinity of the antineutron annihilation detector, is taken up in Secs. IV and V, respectively. Conclusions are drawn in Sec. VI.

II. THE CASE OF A SMALL RESIDUAL MAGNETIC FIELD

For times relevant to ILL-type experiments (which are several orders of magnitude shorter than the lifetime of the neutron), the Pauli-Schrödinger equation for the oscillating neutron-antineutron system in its rest frame reads [62]

$$i\hbar \frac{d}{dt}\begin{pmatrix} \chi_{\mathrm{n}}(t) \\ \chi_{\bar{\mathrm{n}}}(t) \end{pmatrix} = \hbar \begin{pmatrix} \frac{1}{2}\vec{\sigma}\cdot\vec{\omega}_L & \delta \mathbf{1}_2 \\ \delta \mathbf{1}_2 & -\frac{1}{2}\vec{\sigma}\cdot\vec{\omega}_L \end{pmatrix}\begin{pmatrix} \chi_{\mathrm{n}}(t) \\ \chi_{\bar{\mathrm{n}}}(t) \end{pmatrix}, \quad (1)$$

where χ_{n} ($\chi_{\bar{\mathrm{n}}}$) is a neutron (antineutron) Pauli spinor, $\vec{\sigma}$ denotes the triplet of Pauli matrices $\{\sigma_x, \sigma_y, \sigma_z\}$, $\mathbf{1}_2$ is the 2×2 unit matrix, δ is the matrix element of the scalar interaction coupling neutron and antineutron, and, in terms of the residual magnetic field $\vec{B}$ (which is, in general, time dependent), and the negative gyromagnetic ratio γ of the neutron, the Larmor frequency vector $\vec{\omega}_L(t) = -\gamma \vec{B}(t)$ (following the sign convention of Ref. [67]).

In the limit that $\vec{B}$ is strictly uniform and time independent (and, hence, constant in the rest frame), Eq. (1) can be solved exactly to yield the Rabi-like formula for the probability of finding an antineutron at time t after the oscillating state began as a neutron [68,69],

$$P_{\bar{n}}(t) = \frac{\delta^2}{\frac{1}{4}\omega_L^2 + \delta^2}\sin^2\left[\left(\frac{1}{4}\omega_L^2 + \delta^2\right)^{\frac{1}{2}}t\right]. \quad (2)$$

Equation (2) forms the basis for the identification of the *quasifree scaling* regime in which $\omega_L t \ll 1$: under this condition, coupled with the existing empirical bound on δ (which implies that, in all cases of practical interest, $\delta \ll \omega_L$), it follows, from Eq. (2), that $P_{\bar{n}}(t) \approx \delta^2 t^2$, which is identical to the result expected in the absence of any magnetic field.

In the rest frame of the oscillating system, inhomogeneities in $\vec{B}$ translate into explicit time dependence, which, following [62], can be accommodated by working with the interaction picture state vectors

$$\Psi_I(t) = \begin{pmatrix} U_2(t) & 0 \\ 0 & U_2^{\dagger}(t) \end{pmatrix}\begin{pmatrix} \chi_n \\ \chi_{\bar{n}} \end{pmatrix}, \quad (3)$$

where $U_2(t)$ describes evolution of the neutron spinor in the magnetic field $\vec{B}$, i.e.,

$$i\frac{\partial}{\partial t}U_2(t) = \frac{1}{2}\vec{\sigma}\cdot\vec{\omega}_L U_2(t) \quad (4)$$

with $U_2(0) = \mathbf{1}_2$. These interaction picture state vectors satisfy the equation of motion

$$i\hbar \frac{d\Psi_I}{dt} = \hbar\delta\begin{pmatrix} 0 & (U_2^{\dagger}(t))^2 \\ (U_2(t))^2 & 0 \end{pmatrix}\Psi_I. \quad (5)$$

To lowest order in δ, the corresponding probability for detection of an antineutron (with a polarization insensitive detector), starting from a source of unpolarized neutrons at time $t = 0$, is

$$P_{\bar{n}}(t) = \frac{\delta^2}{2}\int_0^t dt' \int_0^t dt'' \mathrm{Tr}[(U_2^{\dagger}(t'))^2(U_2(t''))^2], \quad (6)$$

a result first obtained in Ref. [62] (where the matrix U_2 is denoted by Φ).

Equation (6) permits, in principle, a nonperturbative treatment of the magnetic field, but, in the estimates of the quasifree propagation efficiency of interest, a perturbative calculation suffices. For the purpose of calculating the trace in Eq. (6) to quadratic order in small magnetic fields (equivalently, small $\vec{\omega}_L$), $U_2(t)$ can be approximated as $\exp[-\frac{i}{2}\vec{\varphi}(t)\cdot\vec{\sigma}]$, where the dynamical phase vector

$$\vec{\varphi}(t) \equiv \int_0^t dt' \vec{\omega}_L(t'). \quad (7)$$

To this order in ω_L, Eq. (6) reduces to

$$\frac{P_{\bar{n}}(t)}{\delta^2 t^2} = 1 - \frac{1}{t}\int_0^t dt'\left|\vec{\varphi}(t') - \frac{1}{t}\int_0^t dt''\vec{\varphi}(t'')\right|^2 + \cdots, \quad (8)$$

which is the same as Eq. (18) in Ref. [62].

Allowance can be made for the randomness of the values of magnetic field inhomogeneities sampled in the propagation region by viewing the antineutron detection probability $P_{\bar{n}}$ in Eq. (6) as a functional of a random (or stochastic) process [70], namely, $\vec{\omega}_L(t)$ with the probability distribution functional $\mathcal{P}[\vec{\omega}_L(\cdot)]$. (In what follows, a pair of angle brackets $\langle \cdots \rangle$ will denote an expectation value computed with the probability distribution functional $\mathcal{P}[\vec{\omega}_L(\cdot)]$.) In line with the discussion in the Introduction, it will be assumed that the process $\vec{\omega}_L(t)$ is wide-sense stationary; i.e., the expectation value $\langle \vec{\omega}_L \rangle$ is time independent and the autocorrelation functions

$$\langle (\omega_{L,i}(t_1) - \langle \omega_{L,i} \rangle)(\omega_{L,j}(t_2) - \langle \omega_{L,j} \rangle) \rangle \qquad (9)$$

involving Cartesian components $\omega_{L,i}$ depend only on the relative time difference $t_1 - t_2$.

Under this plausible assumption about the statistics of $\vec{\omega}_L$, the expectation value of the probability in Eq. (8) can be expressed in terms of the sum of the power spectral densities

$$S_{\omega_L}^{(i)}(\omega) = \int_{-\infty}^{+\infty} \langle (\omega_{L,i}(\tau) - \langle \omega_{L,i} \rangle)(\omega_{L,i}(0) - \langle \omega_{L,i} \rangle) \rangle e^{-i\omega\tau} d\tau. \qquad (10)$$

Thus, for example,

$$\left\langle \frac{1}{t} \int_0^t dt' \vec{\varphi}(t') \cdot \vec{\varphi}(t') \right\rangle$$
$$= \frac{1}{3} |\langle \vec{\omega}_L \rangle|^2 t^2 + \frac{1}{\pi} \int_{-\infty}^{+\infty} \frac{d\omega}{\omega^2} [1 - \mathrm{sinc}(\omega t)] S_{\omega_L}(\omega), \qquad (11)$$

where $S_{\omega_L}(\omega) = \sum_i S_{\omega_L}^{(i)}(\omega)$ and $\mathrm{sinc}(x)$ denotes the unnormalized cardinal sine function $[\mathrm{sinc}(x) \equiv \sin(x)/x$ for $x \neq 0$ with $\mathrm{sinc}(0) = 1]$. The complete result for $\langle P_{\bar{n}}(t) \rangle$ reads

$$\frac{\langle P_{\bar{n}}(t) \rangle}{\delta^2 t^2} = 1 - \frac{1}{12} |\langle \vec{\omega}_L \rangle|^2 t^2$$
$$- \frac{1}{2\pi} \int_{-\infty}^{\infty} \frac{d\omega}{\omega^2} \left[1 - \mathrm{sinc}^2 \left(\frac{1}{2} \omega t \right) \right] S_{\omega_L}(\omega) + \cdots. \qquad (12)$$

In the limit of no fluctuations [i.e., $S_{\omega_L}(\omega) \equiv 0$ and $\langle \vec{\omega}_L \rangle = \vec{\omega}_L$], Eq. (12) reduces to the second order perturbative result expected for a small constant magnetic field [which can also be derived directly from Eq. (2)]: the deviation of the ratio $\langle P_{\bar{n}}(t) \rangle/(\delta^2 t^2)$ from unity increases quadratically with increasing time-of-flight t. Equation (12) makes explicit how fluctuations modify this deviation from unity. The associated dependence on t is, in principle, more

complicated than quadratic if $S_{\omega_L}(\omega)$ is not independent of ω.

For the purpose of making numerical estimates, the power spectral densities $S_{\omega_L}^{(i)}(\omega)$ will be taken to be the Lorentzians

$$\frac{2\lambda_i}{1 + \tau_c^2 \omega^2}, \qquad (13)$$

defining wide-sense stationary Markovian noise. Linear superpositions of such Markovian noise sources can model ubiquitous $1/f^\alpha$ noise ($0 < \alpha < 2$) [71,72]. In Eq. (13), τ_c is a correlation time, arising from spatial correlations in the longitudinal (or axial) direction of the propagation region and proportional to the associated correlation length l_c (defined in the laboratory frame). Two choices of l_c, bracketing the range of reasonable values, are adopted in Sec. III: $l_c = 10$ m (about twice the distance between adjacent joints in the shielding used in the ILL experiment) and $l_c = 0$ (the "white" noise limit). The strength λ_i can be related to the statistics of the residual magnetic field by considering the expectation value (with respect to $\mathcal{P}[\vec{\omega}_L(\cdot)]$) of the *square* of

$$\Delta\omega_{L,i} = \frac{1}{t} \int_0^t dt' (\omega_{L,i}(t') - \langle \omega_{L,i} \rangle). \qquad (14)$$

Computation of $\sigma_{L,i}^2 \equiv \langle (\Delta\omega_{L,i})^2 \rangle$ with Eq. (13) (under the assumption of wide-sense stationarity) implies that

$$\lambda_i = \frac{1}{2} \sigma_{L,i}^2 t / \beta\left(\frac{t}{\tau_c} \right) \qquad (15)$$

with $\beta(x) \equiv 1 - (1 - e^{-x})/x$. Equation (12) depends on the combination $\sum_i \lambda_i$ or $\sigma_L^2 \equiv \sum_i \sigma_{L,i}^2$.

In principle, $\langle \omega_{L,i} \rangle$ and $\sigma_{L,i}$ are to be extracted from the detailed comparison of magnetic field profiles along the length of the propagation region. In as much as inhomogeneities in a given profile and changes from one profile to the next both result from the influence of magnetic leaks, it is reasonable to suppose that *estimates* of $\langle \omega_{L,i} \rangle$ and $\sigma_{L,i}$ can be inferred from a *single* profile (of the ith component): $\langle \omega_{L,i} \rangle/\gamma$ and $\sigma_{L,i}/|\gamma|$ should be comparable to the mean and standard deviation, respectively, of the spatial variations in this profile. This assertion can be bolstered by an appeal to the ergodic properties expected of wide-sense stationary random processes (see Sec. IV in Ref. [66]), which imply that the averages over the ensemble of realizations of $\omega_{L,i}$ defining its expectation value and autocorrelation function can be replaced by averages of a typical realization $\omega_{L,i}^{(*)}$ over an infinite time. (Temporal averages in the rest frame become spatial averages in the laboratory frame.)

An eyeballing of field profiles [65] from the ILL experiment (including Fig. 13 in Ref. [63]) suggests that,

except in the vicinity of a few isolated magnetic leaks (considered in Sec. IV), the mean of the residual *axial* field component $B_{\parallel}$ and its standard deviation (about this mean) were reduced to the level of 5 nT or so. There is less information on the transverse components (as the single available profile is corrupted by a magnetized screw), but, because of the coupling between inhomogeneities of axial and transverse components, it can be assumed that their means and standard deviations are similar. In fact, in Ref. [63], it is claimed that the transverse components are smoother than the axial component and that their collective effect is at most equal to that of the axial component—see the discussion immediately preceding Eq. (12) in Ref. [63]. In Sec. III, we set

$$|\langle \vec{\omega}_L \rangle|^2 = 2\gamma^2 (5 \text{ nT})^2 = \sigma_L^2, \qquad (16)$$

corresponding to the conservative selection of a mean of 5 nT and a standard deviation of 5 nT for *both* the axial component $B_{\parallel}$ and the *total* transverse component $B_{\perp}$ of the residual magnetic field $\vec{B}[= \vec{B}_{\parallel} + \vec{B}_{\perp}]$.

III. QUASIFREE PROPAGATION EFFICIENCY ESTIMATES

A figure of merit for the prospects of an ILL-type experiment is proportional to the product $\eta \cdot \langle t^2 \rangle_v$, where the subscripted brackets $\langle \cdots \rangle_v$ denote an average over the neutron time-of-flight spectrum and the quasifree propagation efficiency

$$\eta \equiv \frac{\langle\langle P_{\bar{n}}(t) \rangle\rangle_v}{\delta^2 \langle t^2 \rangle_v}. \qquad (17)$$

Existing studies [4] of the optimal length l of the shielded propagation region for an ILL-type experiment at the ESS have taken into account the increase in $\langle t^2 \rangle_v$ associated with an increase in l. We now investigate the impact on η of an increase in l.

Neutron optics involving supermirrors which redirect neutrons to the annihilation target is crucial to plans for future ILL-type experiments, but, to begin with, it will be supposed that neutrons propagate directly from the source to the target through a fixed horizontal distance l. It will also be assumed that the entirety of this distance is magnetically shielded. (This last assumption is justified in Sec. V.)

Under these assumptions, $\langle P_{\bar{n}}(t) \rangle$ can be re-interpreted as the probability of detecting an antineutron with an axial component v of velocity equal to l/t. One can define an antineutron detection probability which is a function of v: $P_{\bar{n},v}(v) \equiv \langle P_{\bar{n}}(t = l/v) \rangle$. The average $\langle\langle P_{\bar{n}}(t) \rangle\rangle_v$ in Eq. (17) is found by integrating $P_{\bar{n},v}(v)$ over the spectrum of axial speeds.

The total antineutron probability for a propagation region of length l is

$$P_{\bar{n},l} = \langle P_{\bar{n},v}(v) \rangle_v$$
$$\equiv \int_{v_{\min}}^{\infty} P_{\bar{n},v}(v) n(v) dv \int_{v_{\min}}^{\infty} n(v) dv, \qquad (18)$$

where $n(v)$ is the *probability density* for the axial speed v during the experiment and the positive lower limit $v_{\min}$ is the smallest axial speed which is consistent with the requirement that the oscillating neutron-antineutron system, which is in free fall, traverse the *horizontal* propagation region without hitting its tubular walls. (Such collisions have to be avoided for the same reason that the propagation region must be evacuated.) In the quasifree limit, $P_{\bar{n},l}$ reduces to $P_{\bar{n},l}^0 = \delta^2 l^2 \langle v^{-2} \rangle_v$. Thus, the quasifree propagation efficiency is

$$\eta \equiv P_{\bar{n},l}/P_{\bar{n},l}^0$$
$$= \int_{v_{\min}}^{\infty} \frac{P_{\bar{n},v}(v)}{\delta^2 l^2} n(v) dv / \int_{v_{\min}}^{\infty} v^{-2} n(v) dv, \qquad (19)$$

which, on substitution of the expression for $P_{\bar{n},v}(v)$ $[= \langle P_{\bar{n}}(t = l/v) \rangle]$ implied by Eqs. (12), (13), and (15) (with replacement of t and τ_c by l/v and l_c/v, respectively), becomes

$$\eta = 1 - \frac{1}{12} \left[|\langle \vec{\omega}_L \rangle|^2 + 2\tilde{\beta}\left(\frac{l_c}{l}\right) \sigma_L^2 \right] \frac{\mu_{(-4)}}{\mu_{(-2)}} l^2 + \cdots, \qquad (20)$$

where

$$\mu_{(k)} \equiv \int_{v_{\min}}^{\infty} v^k n(v) dv \qquad (21)$$

and $\tilde{\beta}(x) \equiv [1 - 3x + 6x^2 \beta(1/x)]/\beta(1/x)$.

The apparent quadratic dependence of η on l is modified by the factor $\tilde{\beta}(l_c/l)$ and the ratio $\mu_{(-4)}/\mu_{(-2)}$ through its dependence on $v_{\min}$ (see the next paragraph). The function $\tilde{\beta}(x)$, which regulates the contribution of the fluctuation term (i.e., the term containing σ_L^2), is unity for $l_c = 0$ and decreases monotonically as $x = l_c/l$ increases: as one should expect, increasing correlations diminish the effect of fluctuations.

An elementary estimate of the extent free fall (ignoring any influence of the neutron optics) suggests that $v_{\min}$ should be approximately proportional to l, with a constant of proportionality $\alpha \approx (\frac{1}{2}g/d)^{1/2}$, where g is the acceleration due to gravity, and d is the vertical distance through which the oscillating neutron-antineutron system can fall and yet still strike the detector (without interacting with the confining walls of the propagation region). Values of d consistent with current plans (as in Fig. 3 of Ref. [4]) for

future experimental setups range from about 1 m ($\alpha \approx 2.2$ s^{-1}) to about 2 m ($\alpha \approx 1.6$ s^{-1}). Accordingly, in the present investigations, we set $v_{\min} = (1.9$ s$^{-1})l$.

Two quite different choices of $n(v)$ are made. One is the physically motivated superposition

$$n_s(v) = (1-f)\frac{4}{\sqrt{\pi}}\frac{v^2}{v_T^3}\exp\left(-\frac{v^2}{v_T^2}\right) + f\frac{v_c}{v^2}\Theta(v - v_c),$$

$$(22)$$

where f is the epithermal fraction, v_T is the most probable speed for the Maxwellian component, and v_c is the epithermal cutoff speed, parametrized in terms of v_T as $v_c = \sqrt{\mu}v_T$ [73]. (In terms of the absolute temperature T of the Maxwellian, Boltzmann's constant k and the neutron mass m, $v_T = \sqrt{2kT/m}$.) The other more *ad hoc* selection is the Nakagami-like probability density function

$$n_d(v) = \frac{2\Omega^{-\nu}}{\Gamma(\nu)}(v - v_{\min})^{2\nu-1}\exp\left[-\frac{(v - v_{\min})^2}{\Omega}\right]$$

$$\times \Theta(v - v_{\min}),$$

$$(23)$$

where $\Gamma(\nu)$ is the gamma function, and $\Omega = (v_{\max} - v_{\min})^2/(\nu - \frac{1}{2})$, which ensures that $n_d(v)$ peaks at $v = v_{\max}$. For $T = 35$ K (typical of cold neutrons), $\mu = 5$ (advocated in Ref. [73]) and $f = 0.15$ (results are insensitive to an increase or decrease in f by a factor of 3), $n_s(v)$ bears a reasonable resemblance to the simulated spectrum of speeds for the cold neutron source considered in Ref. [4], while, if $v_{\max} = 800$ m/s and $\nu = \frac{3}{2}$, $n_d(v)$ is similar to unpublished simulation results [74] for the speeds of neutrons reaching the detector with neutron optics of the kind outlined in Ref. [4]. The use of both $n_s(v)$ and $n_d(v)$ allows one to gauge the uncertainties in estimates of η due to uncertainties in $n(v)$.

Figure 1 contains plots of the quasifree propagation efficiency η versus shield length l for the four possible pairings of noise model ($l_c = 0$ versus $l_c = 10$ m) with speed spectrum (n_s or n_d). Both the axial and nonaxial components, $\vec{B}_\parallel$ and $\vec{B}_\perp$, respectively, of the magnetic field $\vec{B}$ have a mean and standard deviation of 5 nT [see Eq. (16)]. The ratio of the fluctuation term in Eq. (20) (containing σ_L^2) to the average field term (containing $|\langle\vec{\omega}_L\rangle|^2$) varies from a maximum of 2 when $l_c = 0$ to a minimum of $2\tilde{\beta}(1/5) \approx 1.48$ when $l_c = 10$ m and $l = 50$ m (the minimum value of l in Fig. 1).

With regard to the proposed ILL-type experiment at the ESS, the deliberations in Ref. [4] have not ruled out the possibility that the magnetic field in the propagation region may need to be suppressed to as low as 1 nT. However, it would seem from Fig. 1 that a larger residual magnetic field comparable to that achieved in the ILL experiment can be
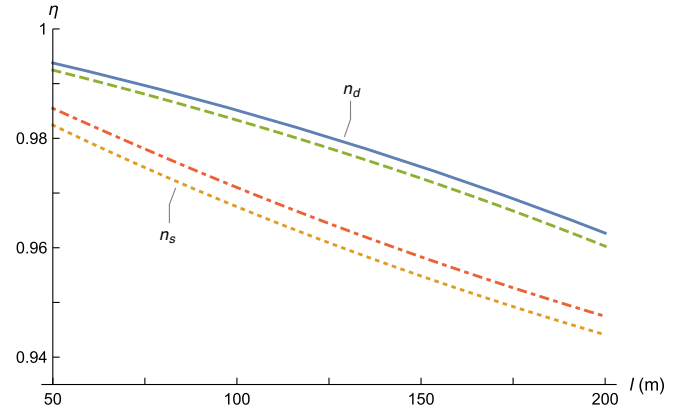

FIG. 1. The quasifree propagation efficiency η versus length l of the propagation region when the mean *and* the standard deviation of the axial component and the *total* transverse component of the residual magnetic field are both equal to 5 nT. The upper (lower) pair of curves corresponds to the harder (softer) spectrum n_d (n_s) of axial speeds. Within each of these pairs of curves, the magnetic fluctuation correlation length $l_c = 10$ m ($l_c = 0$) for the upper (lower) curve. (Parameters of n_s and n_d are given in the text.)

tolerated: η is still in excess of 0.94 for the most interesting values of l, identified as between 175 m and 200 m in Ref. [4]. Although, as anticipated, η decreases with increasing l, the extent of this decrease is sufficiently small ($< 3\%$ as l increases from 100 m to 200 m) that it can be disregarded in any determination of the optimal length of the propagation region.

In view of the quadratic dependence of η in Eq. (20) on magnetic field strength, an improvement by a factor of 2 on the level of field suppression attained in the ILL experiment will be enough to guarantee quasifree propagation efficiencies of more than 98%. Furthermore, given its close proximity to unity, η itself can then be ignored for the purposes of calculating a figure of merit for an ILL-type experiment, as, indeed, it was in Ref. [4].

It is apparent from Fig. 1 that the nature of the axial speed spectrum $n(v)$ has a bigger impact on η than the character of the noise in the residual magnetic field. Another inference from Fig. 1 is that, in lieu of adequate empirical information on either $n(v)$ or the character of the magnetic field noise, one can rely on the estimate of η with white noise ($l_c = 0$) and the Maxwellian-plus-epithermal spectrum $n_s(v)$ to be the most conservative.

The effect of neutron optics has been omitted in the above calculations. The presence of elements like focusing reflectors would mean that there is a range of flight paths for a given time of flight t. However, given the weak and approximately *linear* character of the dependence of η on l, the impact of the dispersion in flight paths on the propagation efficiencies in Fig. 1 should be negligible except for the fact that the abscissa l should be reinterpreted as the *average* flight path.

IV. LOCALIZED LARGE FIELDS AT MAGNETIC LEAKS

In the previous section, the large fields in the immediate vicinity of magnetic leaks in the mumetal shielding were ignored. We now present an argument that justifies neglect of these large fields. It rests largely on the fact that they are localized or, more graphically, "spikelike."

It is convenient to begin with a one-dimensional treatment which takes into account only the axial component of magnetic fields. In this case, the exact solution of Eq. (4) can be obtained in closed form as $U_2(t) = \exp[-\frac{i}{2}\varphi_z(t)\sigma_z]$, where the axial direction within the propagation region has been identified with the z axis [by assumption, $U_2(0)$ is the identity matrix $\mathbf{1}_2$], and Eq. (6) for the probability of an antineutron reduces to [62]

$$P_{\bar{n}}(t) = \delta^2 \left| \int_0^t dt' \exp[i\varphi_z(t')] \right|^2. \qquad (24)$$

The breakout of (axial) magnetic field at points along the shielding can be modeled by replacing the random process $\omega_{L,z}(t)$ by the sum

$$\omega_{L,z}(t) + \sum_{k=1}^N \Delta\varphi_z^k \delta(t - t_k^*), \qquad (25)$$

where $\Delta\varphi_z^k$ denotes the net change in the z component of the dynamical phase across the kth leak (which is encountered at time t_k^* or, in the laboratory frame, at an axial distance l_k^* from the beginning of the propagation region). For neutrons of a given axial component v of velocity, the $\Delta\varphi_z^k$'s can be assumed to be constant during runs of the experiment between any two successive magnetic idealizations of the shield. (Only the process [63] whereby the magnetic shield is idealized is likely to give rise to substantial changes in the $\Delta\varphi_z^k$'s.)

The issue of whether the $\Delta\varphi_z^k$'s in Eq. (25) induce significant corrections to the estimate of η in Eq. (20) can be addressed by considering the maximum value $\Delta\varphi_{max}$ of the $|\Delta\varphi_z^k|$'s. If the largest spike in the axial field attains a value of magnitude B_{max} and has a half-width of Δl, then $\Delta\varphi_{max}$ may be calculated as

$$\Delta\varphi_{max} \approx |\gamma| B_{max} \frac{\Delta l}{v_{min}}$$
$$\approx \Delta\varphi_{max}^{ILL} \left[\frac{v_{min}}{B_{max}} \right]_{ILL} \frac{B_{max}}{v_{min}}$$
$$\approx \Delta\varphi_{max}^{ILL} \left(\frac{D_{ILL}}{D} \right)^{3/2} \frac{l}{l_{ILL}}. \qquad (26)$$

In rewriting $\Delta\varphi_{max}$ in terms of $\Delta\varphi_{max}^{ILL}$, it has been assumed that Δl is not significantly affected by changes in the length l of the shielding, and that, over the relevant range of l,

B_{max} is approximately proportional to $(l/D)^2$ [64,75–77], where D is the diameter of the shielding, while v_{min} is taken to be approximately proportional to $l/D^{1/2}$ (as in the free-fall based estimate of v_{min} earlier).

As regards the configurations for future ILL-type experiments discussed in Ref. [4], even in the worst case contemplated of smallest D and largest l ($D = 2$ m, $l = 200$ m), $\Delta\varphi_{max} \approx 0.9\Delta\varphi_{max}^{ILL}$. Provided *axial* magnetic field profiles resemble those of the ILL experiment, with a few large spikes close to either end of the propagation region, their presence should not be a concern.

In the generalization of these considerations to the *full* magnetic field, one can parallel the discretization method adopted (and tested) in Ref. [78] for the computation of the neutron spinor evolution operator in pulsed fields. Thus, the effect of a spike in the *full* magnetic field on evolution is approximated (at the kth magnetic leak) as a rotation through an angle $\tilde{\varphi}_k$ about a unit vector $\hat{n}_k$. The associated unitary matrix is $U_{2,k} = \exp\left(-\frac{i}{2}\tilde{\varphi}_k \hat{n}_k \cdot \vec{\sigma}\right)$. The reasoning employed in the estimate of $\Delta\varphi_{max}$ above can be repeated to set a bound on the $|\tilde{\varphi}_k|$'s, which, similarly, indicates that they should be smaller for any of the experimental configurations considered in Ref. [4] than in the ILL experiment.

V. MAGNETIC FIELD IN THE VICINITY OF THE DETECTOR

A non-negligible magnetic field ($\gg 1 \mu$T) is unavoidable in the space intervening between the end of the shielded quasifree propagation region and the antineutron detector. In an analysis of the influence of this field, it is appropriate to distinguish between its spatial and temporal average $\vec{B}_{av}$ and fluctuations about $\vec{B}_{av}$. The uniform $\vec{B}_{av}$ can be discussed within the aid of Eq. (24) by the formal device of aligning the z axis with $\vec{B}_{av}$. The fluctuations are assumed to be small in relation to $\vec{B}_{av}$ and are ignored in the present analysis. [A nonperturbative analysis of fluctuations in the axial field based on Eq. (24) shows that there is little or no change in η provided $B_{rms} \lesssim \frac{1}{2}B_{av}$.]

The effect of an uncompensated $\vec{B}_{av}$ can be readily gauged in a model in which the magnitude of the magnetic field has the idealized behavior (in the rest frame) $B(t) = B_{av}\Theta(t - t_{qf})$, where t_{qf} is the time of flight for the quasifree propagation region (of length l_{qf}). Then, beyond the quasifree propagation region ($t > t_{qf}$), the use of Eq. (24) yields

$$\frac{P_{\bar{n}}(t)}{\delta^2 t_{qf}^2} = 1 + \frac{2}{\omega_{av,L} t_{qf}} \sin \omega_{av,L}(t - t_{qf})$$
$$+ \frac{2}{(\omega_{av,L} t_{qf})^2} [1 - \cos \omega_{av,L}(t - t_{qf})], \qquad (27)$$

where $\omega_{av,L} = -\gamma B_{av}$. Deviations from the quasifree scaling term [which is the first term on the right-hand side of Eq. (27)] are negligible, being suppressed by inverse powers of

$$|\omega_{av,L}|t_{qf} > |\omega_{av,L}|\frac{l_{qf}}{v_{min}} = \alpha^{-1}|\omega_{av,L}|\frac{l_{qf}}{l} \sim (10^2/\mu T)B_{av},$$

(28)

where the last product evaluates to a thousand or more for the fields under consideration. In effect, $P_{\bar{n}}(t)$ is frozen at the value $P_{\bar{n}}(t_{qf})$ attained at the end of the interval of quasifree propagation.

As a consequence of the stagnation in the value of $P_{\bar{n}}(t)$, the quasifree propagation efficiency

$$\eta = \eta_{qf}\frac{l_{qf}^2}{l^2}$$

(29)

for $l > l_{qf}$, where η_{qf} is the value of this efficiency at the end of the quasifree propagation region. The l dependence of η in Eq. (29) is stronger than that of η in the quasifree regime for the field strengths adopted in Fig. 1. For example, if $l_{qf} = 175$ m (on average) and the distance of the detector from the end of the magnetically shielded region is 2.8 m (as in the ILL experiment), then, at the location of the detector, $\eta = 0.97\eta_{qf}$. Over a distance of 2.8 m, η has decreased by 3%, whereas, over a quasifree propagation distance of 175 m, η_{qf} decreases by at most 2% (see Fig. 1). Nevertheless, the quantitative difference between η and η_{qf} is sufficiently small that, in any figure of merit, one can, in practice, substitute η by η_{qf}, which is the quantity computed in Sec. III.

VI. CONCLUSION

The investigation of neutron-antineutron oscillations at the ILL in the early 1990s entailed construction of the largest high efficiency magnetically shielded system in existence. In this paper, we have considered what the hard won experience at the ILL suggests about prospects for an even larger shielded system. Concerning the effect of the large spikes in the residual field at the location of unavoidable magnetic leaks in the shielding system, we have presented an argument, relying on little more than reasonable estimates of scaling with system size, that these features can be ignored because they could be ignored in the analysis of the ILL experiment. A calculation admitting magnetic fields of arbitrary strength implies that any large magnetic field encountered after the oscillating

neutron-antineutron system exits the quasifree propagation region (specifically, the field surrounding the detector) will not degrade the probability for antineutron detection. Instead, it is frozen at the value attained at the end of the propagation region. Most of our attention, however, has been focused on a perturbative treatment of the residual field (*sans* spikes) as a random process with the aim of clarifying the relation between the length l of the propagation region and the quasifree propagation efficiency η. Our findings establish that the dependence of η on l is approximately linear (cf. Fig. 1). The overall import of the related numerical estimates of η for values of l relevant to the design of future experiments is encouraging: to attain quasifree propagation efficiencies in excess of 98%, it is enough to improve on the level of magnetic field suppression achieved in the ILL experiment by a mere factor of 2.

Some aspects of our perturbative treatment of η warrant further scrutiny. Variations in the residual magnetic field (after exclusion of any large spikes) have been assumed to be wide-sense stationary. We believe that this assumption is justified for the system under discussion because of the compensation currents deployed, but, nonetheless, its compatibility with data on magnetic field profiles should be tested. Less fundamental to our analysis is the assumption that the magnetic field noise is Markovian, which serves to fix the frequency dependence of the required power spectral densities [cf. Eq. (13)]. It would, of course, be better if power spectral densities taken from experiment were employed, but our results on η suggest that the precise functional form of these densities is unimportant for the estimates made in this paper. More crucial is the ratio of the moments of the axial speed distribution in our final expression for η [in Eq. (20)]. We have attempted to compensate for our ignorance about this ratio by working with two radically different options for the axial speed distribution [given in Eqs. (22) and (23)]. More precise estimates of η require empirical constraints on this ratio of moments.

[1] http://europeanspallationsource.se.
[2] D. A. Milstead, *Proc. Sci.*, EPS-HEP2015 (2015) 603.
[3] C. Theroine, Nucl. Phys. News **25**, 13 (2015).
[4] D. G. Phillips II *et al.*, Phys. Rep. **612**, 1 (2016).
[5] M. J. Frost, arXiv:1607.07271.
[6] M. Baldo-Ceolin *et al.*, Phys. Lett. B **236**, 95 (1990).
[7] M. Baldo-Ceolin *et al.*, Z. Phys. C **63**, 409 (1994).
[8] G. Fidecaro *et al.* (CERN-ILL-Padova-Rutherford-Sussex Collaboration), Phys. Lett. **156B**, 122 (1985).
[9] G. Bressi *et al.*, Z. Phys. C **43**, 175 (1989).
[10] G. Bressi *et al.*, Nuovo Cimento A **103**, 731 (1990).
[11] R. N. Mohapatra, Int. J. Mod. Phys. A **29**, 1430066 (2014).
[12] J. Heeck, Phys. Lett. B **739**, 256 (2014).
[13] A. Addazi, Z. Berezhiani, and Y. Kamyshkov, arXiv:1607.00348.
[14] K. S. Babu and R. N. Mohapatra, Phys. Rev. D **91**, 013008 (2015).
[15] Z. Berezhiani, Eur. Phys. J. C **76**, 705 (2016).
[16] K. S. Babu, R. N. Mohapatra, and S. Nasri, Phys. Rev. Lett. **97**, 131301 (2006).
[17] K. S. Babu, R. N. Mohapatra, and S. Nasri, Phys. Rev. Lett. **98**, 161301 (2007).
[18] K. S. Babu, P. S. Bhupal Dev, and R. N. Mohapatra, Phys. Rev. D **79**, 015017 (2009).
[19] K. S. Babu, P. S. Bhupal Dev, E. C. F. S. Fortes, and R. N. Mohapatra, Phys. Rev. D **87**, 115019 (2013).
[20] S. Patra and P. Pritimita, Eur. Phys. J. C **74**, 3078 (2014).
[21] K. S. Babu and R. N. Mohapatra, Phys. Rev. D **91**, 096009 (2015); **91**, 119905(E) (2015).
[22] K. S. Babu and R. N. Mohapatra, Phys. Rev. D **94**, 054034 (2016).
[23] S. Gardner and E. Jafari, Phys. Rev. D **91**, 096010 (2015).
[24] Z. Berezhiani and A. Vainshtein, arXiv:1506.05096.
[25] K. Fujikawa and A. Tureanu, arXiv:1510.00868.
[26] S. Gardner and X. Yan, Phys. Rev. D **93**, 096008 (2016).
[27] D. McKeen and A. E. Nelson, Phys. Rev. D **94**, 076002 (2016).
[28] V. A. Kuz'min, Pis'ma Zh. Eksp. Teor. Fiz. **12**, 335 (1970) [JETP Lett. **12**, 228 (1970)].
[29] S. L. Glashow, in *Quarks and Leptons: Cargèse 1979*, edited by M. Lévy *et al.* (Plenum Press, New York, 1980), p. 687.
[30] R. N. Mohapatra and R. E. Marshak, Phys. Rev. Lett. **44**, 1316 (1980); **44**, 1644(E) (1980).
[31] T. K. Kuo and S. T. Love, Phys. Rev. Lett. **45**, 93 (1980).
[32] L.-N. Chang and N.-P. Chang, Phys. Rev. Lett. **45**, 1540 (1980).
[33] B. B. Deo, Phys. Lett. **102B**, 267 (1981).
[34] J. F. Nieves, Nucl. Phys. **B189**, 182 (1981).
[35] A. Raychaudhuri and P. Roy, Pramana **19**, 237 (1982).
[36] M. Fukugita, T. Yanagida, and M. Yoshimura, Phys. Lett. **109B**, 369 (1982).
[37] D. Lüst, A. Masiero, and M. Roncadelli, Phys. Rev. D **25**, 3096(R) (1982).
[38] M. Özer, Phys. Rev. D **26**, 3159 (1982).
[39] H. Harari, R. N. Mohapatra, and N. Seiberg, Nucl. Phys. **B209**, 174 (1982).
[40] G. Costa, F. Feruglio, and F. Zwirner, Nucl. Phys. **B209**, 183 (1982).
[41] S. Rao and R. E. Shrock, Phys. Lett. **116B**, 238 (1982).
[42] S. Rao and R. E. Shrock, Nucl. Phys. **B232**, 143 (1984).
[43] K. Babu *et al.* (NNbarX Collaboration), arXiv:1310.8593.
[44] P. Fileviez Pérez, Phys. Rep. **597**, 1 (2015).
[45] J. M. Arnold, B. Fornal, and M. B. Wise, Phys. Rev. D **87**, 075004 (2013).
[46] B. Fornal, Ph.D. thesis, California Institute of Technology, 2014, http://resolver.caltech.edu/CaltechTHESIS:04082014-225653991.
[47] L. Calibbi, G. Ferretti, D. Milstead, C. Petersson, and R. Pöttgen, J. High Energy Phys. 05 (2016) 144.
[48] A. Martin and G. C. Stavenga, Phys. Rev. D **85**, 095010 (2012).
[49] M. I. Buchoff, C. Schroeder, and J. Wasem, *Proc. Sci.*, LATTICE2012 (2012) 128.
[50] M. I. Buchoff and M. Wagman, Phys. Rev. D **93**, 016005 (2016).
[51] S. Syritsyn, M. I. Buchoff, C. Schroeder, and J. Wasem, *Proc. Sci.*, LATTICE2015 (2015) 132.
[52] S. Nussinov and R. Shrock, Phys. Rev. Lett. **88**, 171601 (2002).
[53] E. Herrmann, arXiv:1408.4455.
[54] A. Addazi and M. Bianchi, J. High Energy Phys. 12 (2014) 089.
[55] D. T. Brennan, arXiv:1503.08849.
[56] A. Karozas, S. F. King, G. K. Leontaris, and A. K. Meadowcroft, J. High Energy Phys. 10 (2015) 041.
[57] A. Addazi, Phys. Lett. B **757**, 462 (2016).
[58] A. Addazi, M. Bianchi, and G. Ricciardi, J. High Energy Phys. 02 (2016) 035.
[59] A. Addazi, J. Valle, and C. Vaquera-Araujo, Phys. Lett. B **759**, 471 (2016).
[60] P. Gu, E. Ma, and U. Sarkar, Phys. Rev. D **94**, 111701(R) (2016).
[61] M. C. Ramáo, A. Karozas, S. F. King, G. K. Leontaris, and A. K. Meadowcroft, J. High Energy Phys. 11 (2016) 081.
[62] U. Kinkel, Z. Phys. C **54**, 573 (1992).
[63] T. Bitter *et al.*, Nucl. Instrum. Methods Phys. Res., Sect. A **309**, 521 (1991).
[64] S. Dickerson, J. M. Hogan, D. M. S. Johnson, T. Kovachy, A. Sugarbaker, S. Chiow, and M. A. Kasevich, Rev. Sci. Instrum. **83**, 065108 (2012).
[65] D. Dubbers (private communication).
[66] A. M. Yaglom, *An Introduction to the Theory of Stationary Random Functions* (Prentice-Hall, Englewood Cliffs, NJ, 1962).
[67] M. H. Levitt, *Spin Dynamics: Basics of Nuclear Magnetic Resonance* (John Wiley & Sons, Chichester, 2008).
[68] R. N. Mohapatra and R. E. Marshak, Phys. Lett. **94B**, 183 (1980).
[69] R. A. Arndt, V. B. Prasad, and Riazuddin, Phys. Rev. D **24**, 1431(R) (1981).
[70] C. W. Gardiner, *Stochastic Methods: A Handbook for the Natural and Social Sciences* (Springer, Berlin, Heidelberg, 2009).
[71] P. Kuopanportti, M. Möttönen, V. Bergholm, O.-P. Saira, J. Zhang, and K. B. Whaley, Phys. Rev. A **77**, 032334 (2008).
[72] D. J. Gorman, K. C. Young, and K. B. Whaley, Phys. Rev. A **86**, 012317 (2012).

[73] C. R. Gould, E. I. Sharapov, and S. K. Lamoreaux, Phys. Rev. C **74**, 024607 (2006).

[74] W. M. Snow, Neutron-Anti-Neutron Oscillations at ESS, CERN, Geneva, Switzerland, 2014, http://indico.esss.lu.se/event/171/session/1/contribution/24/material/slides/0.pdf.

[75] A. Mager, IEEE Trans. Magn. **6**, 67 (1970).

[76] D.-X. Chen, E. Pardo, and A. Sanchez, J. Magn. Magn. Mater. **306**, 135 (2006).

[77] X. Sun, L. Jiang, and P. W. T. Pong, Microelectron. Eng. **111**, 77 (2013).

[78] F. M. Piegsa, Nucl. Instrum. Methods Phys. Res., Sect. A **786**, 71 (2015).